

LETTERS

A Theoretical Study of $\text{ClONO}_2 + \text{Cl}^- \rightarrow \text{Cl}_2 + \text{NO}_3^-$ on Ice

Roberto Bianco*[†] and James T. Hynes*^{†,‡}

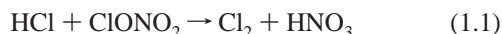
*Department of Chemistry and Biochemistry, University of Colorado, Boulder, Colorado 80309-0215, and
Département de Chimie, CNRS UMR 8640 PASTEUR, Ecole Normale Supérieure, 24 rue Lhomond,
Paris 75231, France*

Received: January 22, 2003; In Final Form: April 1, 2003

The title reaction, of interest in connection with the central heterogeneous reaction $\text{HCl} + \text{ClONO}_2 \rightarrow \text{Cl}_2 + \text{HNO}_3$ for polar stratospheric ozone depletion, is studied quantum chemically at the Hartree–Fock level via a $\text{Cl}^- \cdot \text{ClONO}_2$ complex anion embedded in a model ice lattice $\text{Cl}^- \cdot \text{ClONO}_2 \cdot (\text{H}_2\text{O})_8 \cdot \text{W}_{29}$ comprising both quantum chemical and classical polarizable water molecules (W). The calculated reaction mechanism involves the nucleophilic attack of Cl^- on the electrophilic $\text{Cl}^{\delta+}$ in ClONO_2 , assisted by changes in hydrogen bonding involving both the desolvation of Cl^- and the increased solvation of the nitrate group. The calculated reaction barrier at 0 K, including the zero-point energy correction, is 5.7 kcal/mol. This result is compared with previous results for the $\text{HCl} + \text{ClONO}_2 \rightarrow \text{Cl}_2 + \text{HNO}_3$ reaction (Bianco, R.; Hynes, J. T. *J. Phys. Chem. A* **1999**, *103*, 3797), and implications for stratospheric heterogeneous chemistry are discussed.

1. Introduction

The production of photolyzable chlorine (Cl_2) from chlorine nitrate (ClONO_2) and hydrochloric acid (HCl) on stratospheric aerosols via the bimolecular nucleophilic substitution ($\text{S}_{\text{N}}2$) reaction

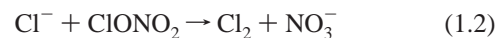


is an efficient heterogeneous process¹ that greatly influences seasonal ozone depletion in the Antarctic stratosphere^{2,3} under acidic conditions.^{4–7}

We have proposed a mechanism for reaction 1.1 on pure ice based on quantum chemical calculations on a $\text{HCl} \cdot \text{ClONO}_2 \cdot (\text{H}_2\text{O})_9$ model reaction system.⁸ A natural assumption of that study was that the hydronium ion, which was found to be formed in the dissociation of HCl, remains in close proximity to the

reactants during the surface reaction. The nucleophilic attack of Cl^- on the electrophilic chlorine in ClONO_2 was shown⁸ to be assisted by proton transfer from the hydronium ion of the $\text{H}_3\text{O}^+ \cdot \text{Cl}^-$ contact ion pair within the ice lattice to a surface water coordinated to ClONO_2 , to form a new contact ion pair with the ensuing nitrate anion; a similar set of proton transfers in the ice lattice was found earlier for the hydrolysis of ClONO_2 .⁹ The results indicated a barrier of about 6.4 kcal/mol (inclusive of the zero-point energy correction) for this coupled proton transfer– $\text{S}_{\text{N}}2$ reaction.⁸ This proton transfer-assisted mechanism was subsequently supported by ref 10.

However, as stressed in ref 8, it is also important to consider the reaction



similar to reaction 1.1, in which the hydronium ion is not present. This reaction was studied in the gas phase by Haas et al.¹¹ and was shown to be barrierless both experimentally and via quantum chemical calculations on the $\text{Cl}^- \cdot \text{ClONO}_2$ com-

* Corresponding authors. E-mail: roberto.bianco@colorado.edu, hynes@spot.colorado.edu. Fax: +303 492 5894.

[†] University of Colorado.

[‡] Ecole Normale Supérieure.

plex: a $\text{Cl}_2\cdot\text{NO}_3^-$ product complex forms spontaneously from the reactants. In an attempt to model solvation effects in ref 11, calculations of the reaction energetics via a dielectric continuum model indicated that the heterogeneous realization of reaction 1.2 would also be exothermic. However, as noted in ref 11, the lack of assessment of the reaction barrier rendered the investigation inconclusive as to the viability of reaction 1.2 on ice.

In view of the efficiency of reaction 1.2 in the gas phase, one might argue that if the acidic proton in heterogeneous reaction 1.1 diffused sufficiently far from the reaction site, then reaction 1.2 might actually produce Cl_2 more efficiently than reaction 1.1. The validity of such an argument, however, is not at all clear. As to be discussed further within, key features of the barrier height for reaction 1.2 include both the desolvation of Cl^- and the increased solvation of the nitrate group, well-known aspects of $\text{S}_{\text{N}}2$ reactions.^{12,13} As previously highlighted for reaction 1.1 in ref 8, both the nucleophilic attack and its coupled proton transfer involve, at the transition state, the delocalization of the $\text{Cl}^- \cdot \text{H}_3\text{O}^+$ contact ion pair charges on the $[\text{Cl}\cdots\text{Cl}\cdots\text{ONO}_2]^-$ group and a $[\text{H}_2\text{O}\cdots\text{H}\cdots\text{OH}_2]^+$ cation, respectively. But whereas the delocalization of the negative charge is a feature common to both reactions 1.1 and 1.2, that of the positive charge, from a standard solvation perspective, involves an additional barrier-increasing effect for 1.1 compared to 1.2. Such a view, however, ignores the proton's important assisting electronic effects for reaction 1.1.⁸ A detailed investigation of the alternative pathway 1.2 would thus shed further light on the role of proton transfer in these heterogeneous reactions. To our knowledge, there has been no study addressing either the microscopic mechanism for the heterogeneous version of 1.2 or the competition between 1.1 and 1.2, both of which are the subjects of this investigation.

The outline of the remainder of this paper is as follows. In section 2, we discuss the selection of the model reaction system and the computational strategy. Highlights from the reaction path are presented in section 3, and concluding remarks are offered in section 4 and are focused on the comparison of reactions 1.1 and 1.2 in a stratospheric context with attention to the issue^{8,14} of whether the proton remains in proximity of Cl^- at the ice surface.

2. Model Reaction System and Computational Method

Our computational strategy was informed by the following considerations. Reaction 1.2 is an $\text{S}_{\text{N}}2$ reaction, with the waters in the ice lattice having a purely solvating function. Assuming that ClONO_2 does not penetrate into the ice lattice, the Cl^- anion has to be positioned at the surface for the reaction to occur, hydrogen bonded to three surface waters, and coordinated to the electrophilic chlorine in ClONO_2 .^{9,15,16} The oxygens of the nitrate group are also hydrogen bonded to the surface waters. (Below, we will loosely refer to these solvating waters hydrogen bonded to either Cl^- or ClONO_2 as the first solvation shell.) The entire reactant complex (RC) is consistent with ClONO_2 situated on an ice lattice in which HCl has ionized,¹⁷ but in contrast to our previous study of reaction 1.1,⁸ we assume that the proton arising from the HCl ionization has diffused far from the reaction site.

Stemming from these considerations and in a fashion similar to our previous studies of ClONO_2 reactions on ice surfaces,^{8,9,15} we have modeled reaction 1.2 using an assembly comprising (a) the $\text{Cl}^- \cdot \text{ClONO}_2$ core reaction system (CRS) described quantum chemically; (b) the CRS' first solvation shell comprising 8 waters, also described quantum chemically; and (c) a

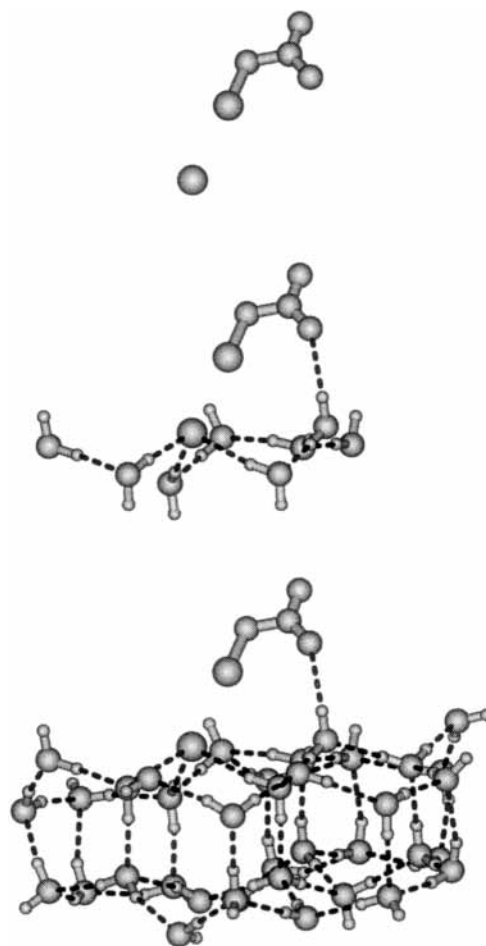


Figure 1. Schematics of the model reaction system and embedding process: (i) top, $\text{Cl}^- \cdot \text{ClONO}_2$ complex; (ii) middle, $\text{Cl}^- \cdot \text{ClONO}_2 \cdot (\text{H}_2\text{O})_8$ core reaction system; (iii) bottom, $\text{Cl}^- \cdot \text{ClONO}_2 \cdot (\text{H}_2\text{O})_8 \cdot \text{W}_{29}$ model reaction system, which was used in the calculations.

hexagonal ice lattice assembled around the waters in the first solvation shell of the CRS and composed of 29 classical polarizable waters. The embedding procedure implements an algorithm for the construction of a hexagonal ice lattice proposed in ref 18. Initially, an ice slab of a size adequate to naturally constrain the CRS was assembled by positioning the ice oxygens but without assigning the hydrogens. One O in the center of the top monolayer was replaced with Cl^- , and the hydrogens in the surface CRS $(\text{H}_2\text{O})_8$ cluster were assigned manually to hydrogen-bond Cl^- and provide a dangling OH bond for the coordination of ClONO_2 , which was positioned last. Some of the waters not coordinated to either Cl^- or ClONO_2 were oriented with dangling OH bonds to hydrogen-bond to the ensuing NO_3^- ion. At this stage, the H's in the rest of the lattice were assigned randomly, shell by shell, propagating from the $(\text{H}_2\text{O})_8$ quantum cluster, with one exception: The H's of the n waters directly coordinated to $(\text{H}_2\text{O})_8$ were assigned to minimize the $\text{Cl}^- \cdot \text{ClONO}_2 \cdot (\text{H}_2\text{O})_8 \cdot \text{W}_n$ dipole moment. The complexity of the model reaction system is illustrated by the deconstructed view of the optimized RC in Figure 1, which also highlights the embedding process.

GAMESS¹⁹ was used for the quantum chemical calculations. For the initial exploration of the potential energy surface, we have used the Hay–Wadt (HW) effective core potential (ECP) basis set²⁰ complemented by polarization (“d”, Cl exp 0.75,²¹ O, N exp 0.8²¹) and diffuse (“+”, Cl exp. 0.0483,²² O exp. 0.0845, N exp. 0.0639²³) functions on the $\text{Cl}^- \cdot \text{ClONO}_2 \cdot (\text{H}_2\text{O})_8$ CRS cluster's heavy atoms. GAMESS provides a representation

TABLE 1: Relevant Parameters for the Reactant Complex, Transition State, and Product Complex^a

	RC	TS	PC
ΔE	0.	6.6	-9.8
ΔE w/ZPE	0.	5.7	-10.7
Cl \cdots Cl'	2.91	2.28	1.99
Cl' \cdots ONO ₂	1.69	1.95	2.99
(H ₂ O) ₃ \cdots Cl	2.25	2.46	3.70
ONO ₂ \cdots (H ₂ O) ₃	4.04	2.64	1.93
$q(\text{Cl})$	-0.81	-0.50	-0.06
$q(\text{Cl}')$	0.44	0.29	-0.02
$q(\text{ONO}_2)$	-0.59	-0.87	-1.07

^a RC: reactant complex. TS: transition state. PC: product complex. ΔE : energy difference at 0 K referenced to RC in kcal/mol. ΔE w/ZPE: energy difference at 0 K including zero-point energy correction referenced to RC in kcal/mol. Cl \cdots Cl': distance in Å between the attacking chloride and the chlorine in ClONO₂. Cl' \cdots ONO₂: distance in Å between chlorine and oxygen in ClONO₂. (H₂O)₃ \cdots Cl: average hydrogen bond length in Å between the attacking Cl⁻ and its three solvating waters. ONO₂ \cdots (H₂O)₃: average hydrogen bond length in Å between the nitrate group and its three solvating waters. $q(\text{Cl})$, $q(\text{Cl}')$, $q(\text{ONO}_2)$: Löwdin charges in e .

of classical polarizable waters in terms of effective fragment potentials (EFPs),²⁴ also indicated as "W" below. The EFPs' internal structure is frozen.

All calculations were executed at the Hartree-Fock (HF) level in the following steps. First, the Cl⁻·ClONO₂·(H₂O)₈·W₂₉ RC was optimized. Then, starting from the RC, the transition state (TS) was located via the procedure used in refs 8 and 9 by reducing the Cl \cdots Cl distance in a stepwise fashion and constraining it while optimizing all of the other internal coordinates of the Cl⁻·ClONO₂·(H₂O)₈·W₂₉ cluster before launching the TS full optimization. The W₂₉ lattice was also optimized.

Next, starting from the HF/[HW+(d),EFP]-optimized TS structure, we located the HF/[SBK+(d),EFP]-optimized TS, where the heavy atoms were described by the larger Stevens-Bash-Krauss (SBK)²⁵ ECP basis set. For this calculation, only the atoms in the Cl⁻·ClONO₂ moiety were complemented by polarization and diffuse functions, with the same exponents used for the HW basis set. The SBK+(d) basis set is comparable to the DH(d,p) basis set used to parametrize the water EFPs.²⁴

Finally, starting from the HF/[SBK+(d),EFP] TS, we have calculated the intrinsic reaction coordinate path backward to the RC and forward to the product complex (PC) and have obtained the internal energy barrier and exothermicity at 0 K.

3. Cl⁻·ClONO₂·(H₂O)₈·W₂₉ → Cl₂·ONO₂⁻·(H₂O)₈·W₂₉

The optimized structures of the reactant complex (RC), transition state (TS), and product complex (PC) are shown in Figures 2–4, respectively, with their relevant structural parameters reported in Table 1. The W₂₉ lattice is omitted from the Figures to allow a better appreciation of the structural features of the CRS along the reaction path. We now discuss these structures in turn.

In Figure 2 for the RC, Cl⁻ is fully coordinated to both the lattice and ClONO₂, with the latter also hydrogen bonded to a dangling OH bond. ClONO₂ is planar and polarized, although not ionized into Cl⁺ and ONO₂⁻, consistent with our findings for ClONO₂ in related environments.^{8,9,26} On average, the three hydrogen bonds on Cl⁻ at 2.25 Å (cf. Table 1) are shorter than those to the oxygens of the nitrate group at 4.04 Å. The charge distribution shows a Cl⁻ center (-0.81 e) that has transferred some of its electronic charge to the surrounding species.

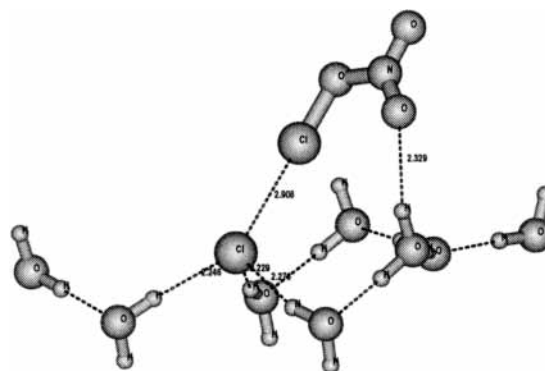


Figure 2. Cl⁻·ClONO₂·(H₂O)₈·W₂₉ reactant complex (RC) at the HF/[SBK+(d),EFP] level. Bond lengths are in Å. The embedding water lattice is not shown.

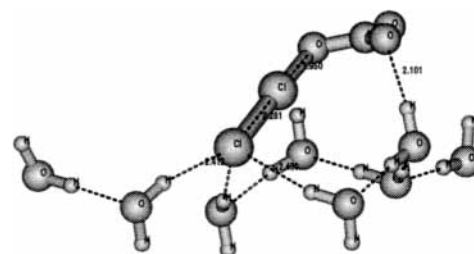


Figure 3. [Cl⁻·Cl⁻·Cl⁻·ONO₂]⁻·(H₂O)₈·W₂₉ transition state (TS) at the HF/[SBK+(d),EFP] level. Bond lengths are in Å. The embedding water lattice is not shown.

At the TS (cf. Figure 3 and Table 1), the Cl-Cl bond has been significantly shortened to 2.28 from 2.91 Å in the RC, and the Cl-O bond in ClONO₂ has lengthened to 1.95 from 1.69 Å in the RC. In addition, the length of the average hydrogen bond to the attacking Cl⁻ has increased to 2.46 Å (from 2.25 Å), whereas that to the nitrate group has significantly decreased to 2.64 Å, consistent with its charge decrease from -0.59 e to -0.87 e . These features indicate that Cl⁻ electron density is engaged in Cl-Cl bond formation and is therefore less available for hydrogen bonding to the ice lattice, and also that the increased electron density on the ensuing NO₃⁻ ion is strengthening the hydrogen bonds to this group by the lattice waters. Alternatively stated, compared to the RC, the TS is characterized by the desolvation of the attacking Cl⁻ and increased solvation of the leaving NO₃⁻ moiety. Furthermore, the ClONO₂ has lost the planarity originally present in the RC, signaling a decrease in the ClO-NO₂ double-bond character. The changes in atomic charge distribution further emphasize the electron transfer from Cl⁻ to NO₃⁻.

The reaction barrier at 0 K is calculated to be 6.6 kcal/mol, with an exothermicity of -9.8 kcal/mol. By including the zero-point energy (ZPE) correction, the barrier is lowered to 5.7 kcal/mol, and the exothermicity increases to -10.7 kcal/mol. Previous estimates of the reaction enthalpy of 1.2 were -14 and -5 kcal/mol.¹¹

In the product complex (cf. Figure 4), the NO₃⁻ ion is more strongly hydrogen-bonded to the ice surface, with an average hydrogen bond length of 1.93 Å, whereas the newly formed Cl₂ has retained only a weak interaction with NO₃⁻, with a Cl₂ \cdots ONO₂⁻ distance of 2.99 Å. The average hydrogen bond length to the original Cl⁻ has increased to 3.70 Å.

We note that the calculated internal energies above do not include electron correlation because of the HF-level parametrization of the EFPs.²⁴ Since the inclusion of electron correlation for the companion HCl + ClONO₂ reaction 1.1 slightly increased its barrier by only about 0.4 kcal/mol with respect to

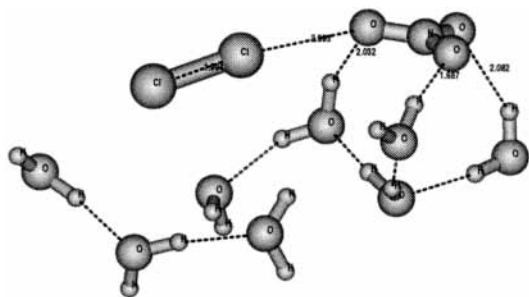


Figure 4. $\text{Cl}_2\cdot\text{ONO}_2\cdot(\text{H}_2\text{O})_8\cdot\text{W}_{29}$ product complex (PC) at the HF/[SBK+(d),EFP] level. Bond lengths are in Å. The embedding water lattice is not shown.

that of the HF calculation (cf. ref 8, Figure 2, panel a), we consider the current HF-level barrier for reaction 1.2 to be a reliable quantity.

4. Concluding Remarks

The Hartree–Fock-level electronic structure calculations presented within indicate that the $\text{Cl}^- + \text{ClONO}_2 \rightarrow \text{Cl}_2 + \text{NO}_3^-$ reaction at the surface of ice will proceed via an $\text{S}_{\text{N}}2$ reaction mechanism, with an estimated barrier height of 6.6 kcal/mol (5.7 kcal/mol including ZPE) and an exothermicity of -9.8 kcal/mol (-10.7 kcal/mol including ZPE). This barrier height is comparable to that (6.4 kcal/mol including ZPE) previously estimated⁸ for the $\text{HCl} + \text{ClONO}_2 \rightarrow \text{Cl}_2 + \text{HNO}_3$ reaction on ice, where proton transfer in the ice lattice is actively involved. Within the uncertainties of the calculations, then, there is no obvious preference for one reaction path over the other in the polar stratospheric context, so that the issue becomes that of whether the hydronium ion produced in the HCl acid ionization has its proton transported away from the Cl^- ion that then attacks the chlorine nitrate at the ice surface at 190 K. We note, however, that it has been suggested that the ClONO_2 reaction in the polar stratosphere may actually occur at the surface of acidic sulfate aerosols,^{1,27} in which case the proton-assisted reaction 1.1 would appear to be more likely (as it would be on an acidified ice surface).

Experimental investigations on related proton-transport problems have reached opposing conclusions. Reflection absorption infrared spectroscopic studies of HCl taken up at one surface of an ice sample have indicated the appearance of H_3O^+ at the opposite surface of the sample,²⁸ and experiments on soft-landed protons have been interpreted as indicating no transport of the proton away from the surface region at 30–190 K.¹⁴ (The latter experiments, however, do not address the lateral surface transport of the proton.) Earlier experimental results indicating limited uptake of HCl on ice surfaces at 190 K suggest^{4,17} that any ionized HCl would stay in the surface region. In view of these results, it would be of interest to examine this proton-transport issue theoretically in the context of the $\text{HCl} + \text{ClONO}_2$ reaction on ice.

As we have previously suggested,⁸ comparison isotopic substitution experiments involving DCl and D_2O ice could be useful in distinguishing whether the chlorine nitrate reaction occurs in the presence or absence of the proton. One would expect significant effects for reaction 1.1 involving the proton²⁹ but not for current reaction 1.2.³⁰ In this connection, one must consider issues of product desorption, now discussed. We have argued previously⁸ that an H/D isotope effect is probably not observable for the ClONO_2 hydrolysis on ice despite the proposed proton-transfer involvement⁹ because of the HOCl desorption energy (ca. 13 kcal/mol)⁴ exceeding the calculated reaction barrier of ~ 3 kcal/mol;⁹ then the surface reaction would

not be rate-limiting. The observed lack of an H/D isotope effect for ClONO_2 hydrolysis on D_2O ice supports this view.³¹ For reaction 1.1, however, Cl_2 dissociation from the ice with accompanying increased NO_3^- solvation is exothermic (see text and ref 11), with the mechanism at a dynamic surface^{17,32} likely being the simple exchange of an H_2O for the Cl_2 in the NO_3^- solvation shell. Thus, the barrier should be low to modest, such that the overall rate would still depend on the rate of 1.1, with a resulting finite kinetic isotope effect.⁸

Acknowledgment. This work was supported by NSF grants ATM-9613802 and ATM-0000542. This research was performed, in part, using the Molecular Science Computing Facility (MSCF) in the William R. Wiley Environmental Molecular Sciences Laboratory, a national scientific user facility sponsored by the U.S. Department of Energy's Office of Biological and Environmental Research and located at the Pacific Northwest National Laboratory. Pacific Northwest is operated for the Department of Energy by Battelle.

Supporting Information Available: Structures, energies, and vibrational frequencies of the transition state, reactant complex, and product complex of the $\text{Cl}^- \cdot \text{ClONO}_2 \cdot (\text{H}_2\text{O})_8 \cdot (\text{EFP})_{29}$ model reaction system. This material is available free of charge via the Internet at <http://pubs.acs.org>.

References and Notes

- (1) Solomon, S. *Rev. Geophys.* **1988**, *26*, 131.
- (2) Solomon, S.; Garcia, R. R.; Rowland, F. S.; Wuebbles, D. J. *Nature* **1986**, *321*, 755. Solomon, S. *Nature* **1990**, *347*, 347.
- (3) For reviews, see Brune, W. H.; Anderson, J. G.; Toohey, D. W.; Fahey, D. W.; Kawa, S. R.; Jones, R. L.; McKenna, D. S.; Poole, L. R. *Science* **1991**, *252*, 1260. Anderson, J. G.; Toohey, D. W.; Brune, W. H. *Science* **1991**, *251*, 39. Schoeberl, M. R.; Hartmann, D. L. *Science* **1991**, *251*, 46.
- (4) Hanson, D. R.; Ravishankara, A. R. *J. Phys. Chem.* **1992**, *96*, 2682.
- (5) Chu, L. T.; Leu, M.-T.; Keyser, L. F. *J. Phys. Chem.* **1993**, *97*, 12798.
- (6) Oppliger, R.; Allan, A.; Rossi, M. J. *J. Phys. Chem. A* **1997**, *101*, 1903.
- (7) Horn, A. B.; Sodeau, J. R.; Roddis, T. B.; Williams, N. A. *J. Phys. Chem. A* **1998**, *102*, 6107.
- (8) Bianco, R.; Hynes, J. T. *J. Phys. Chem. A* **1999**, *103*, 3797.
- (9) Bianco, R.; Hynes, J. T. *J. Phys. Chem. A* **1998**, *102*, 309.
- (10) McNamara, J. P.; Tresadern, G.; Hillier, I. H. *J. Phys. Chem. A* **2000**, *104*, 4030.
- (11) Haas, B.-M.; Crellin, K. C.; Kuwata, K. T.; Okumura, M. *J. Phys. Chem.* **1994**, *98*, 6740.
- (12) Gertner, B. J.; Whitnell, R. M.; Wilson, K. R.; Hynes, J. T. *J. Am. Chem. Soc.* **1991**, *113*, 74.
- (13) See, for example, Chandrasekhar, J.; Smith, S. F.; Jorgensen, W. L. *J. Am. Chem. Soc.* **1984**, *106*, 3049. Chandrasekhar, J.; Smith, S. F.; Jorgensen, W. L. *J. Am. Chem. Soc.* **1985**, *107*, 154.
- (14) Cowin, J. P.; Tsekouras, A. A.; Iedema, M. J.; Wu, K.; Ellison, G. B. *Nature* **1999**, *398*, 405.
- (15) Bianco, R.; Gertner, B. J.; Hynes, J. T. *Ber. Bunsen-Ges. Phys. Chem.* **1998**, *102*, 518.
- (16) Lee, T. J. *J. Phys. Chem.* **1995**, *99*, 1943.
- (17) Gertner, B. J.; Hynes, J. T. *Science* **1996**, *271*, 1563. Gertner, B. J.; Hynes, J. T. *Faraday Discuss.* **1998**, *110*, 301. See also Clary, D. C.; Wang, L. *J. Chem. Soc., Faraday Trans.* **1997**, *93*, 2763.
- (18) Hayward, J. A.; Reimers, J. R. *J. Chem. Phys.* **1997**, *106*, 1518.
- (19) Schmidt, M. W.; Baldrige, K. K.; Boatz, J. A.; Elbert, S. T.; Gordon, M. S.; Jensen, J. J.; Koseki, S.; Matsunaga, N.; Nguyen, K. A.; Su, S.; Windus, T. L.; Dupuis, M.; Montgomery, J. A. *J. Comput. Chem.* **1993**, *14*, 1347.
- (20) Hay, P. J.; Wadt, W. R. *J. Chem. Phys.* **1985**, *82*, 270.
- (21) Pietro, W. J.; Francl, M. M.; Hehre, W. J.; DeFrees, D. J.; Pople, J. A.; Binkley, J. S. *J. Am. Chem. Soc.* **1982**, *104*, 5039.
- (22) Spitznagel, G. W. Diplomarbeit, Erlangen, 1982.
- (23) Clark, T.; Chandrasekhar, J.; Spitznagel, G. W.; von R. Schleyer, P. *J. Comput. Chem.* **1983**, *4*, 294.
- (24) Day, P. N.; Jensen, J. H.; Gordon, M. S.; Webb, S. P.; Stevens, W. J.; Krauss, M.; Garmer, D.; Basch, H.; Cohen, D. *J. Chem. Phys.* **1996**, *105*, 1968. Chen, W.; Gordon, M. S. *J. Chem. Phys.* **1996**, *105*, 11081.

(25) Stevens, W. J.; Bash, H.; Krauss, M. *J. Chem. Phys.* **1984**, *81*, 6026.

(26) Bianco, R.; Thompson, W. H.; Morita, A.; Hynes, J. T. *J. Phys. Chem. A* **2001**, *105*, 3132.

(27) See Hanson, D. R. *J. Phys. Chem. A* **1998**, *102*, 4794 for a detailed experimental study of the reaction on sulfate aerosol model surfaces.

(28) Donsig, H. A.; Vickerman, J. C. *J. Chem. Soc., Faraday Trans.* **1997**, *93*, 2755. Horn, A. B.; Sully, J. *J. Chem. Soc., Faraday Trans.* **1997**, *93*, 2741.

(29) A more complete theoretical treatment of eq 1.2 than that provided in ref 8 would include the quantization of the proton's (deuteron's) nuclear motion. See Ando, K.; Hynes, J. T. *Adv. Chem. Phys.* **1999**, *110*, 381.

(30) Differential solvation effects of H₂O and D₂O (Marcus, Y. *Solvation*; Wiley & Sons: New York, 1985) would require attention in this connection.

(31) Hanson, D. R. Personal communication.

(32) Haynes, D. R.; Tro, N. J.; George, S. M. *J. Phys. Chem.* **1992**, *96*, 8502.